Green Chemistry

PAPER

View Article Online
View Journal

Cite this: DOI: 10.1039/d5gc03955j

High energy content bi- and mono-cycloalkane and iso-alkane jet blending mixtures derived from ethanol

Robert A. Dagle,*[a] Nickolas Riedel,[a] Zhibin Yang,[b] Johnny Saavedra Lopez,[a] Alia Cooper,[a] Michael Thorson,[a] Louis Edwards Caceres-Martinez,[c] Wan Tang Jeff Zhang,[c] Hilkka I. Kenttämaa,[d] Gozdem Kilaz,[c] Joshua Heyne[a,b] and Ralph Gillespie[e]

This study introduces two novel alcohol-to-jet catalytic pathways, both yielding a cycloalkane-rich liquid product with the potential to enhance fuel performance beyond current synthetic jet blendstocks. The process begins with ethanol-derived butene, which is converted into gasoline-range aromatics. The resulting aromatic intermediate is then upgraded into the jet-range fraction through two distinct approaches: alkylation, which produces alkyl-substituted aromatics, and hydroalkylation, which generates dual-ring cyclic compounds. Both products undergo selective hydrogenation, demonstrating minimal product loss due to undesirable cracking or ring-opening reactions. After distillation into the jet-range fraction, the alkylated and hydroalkylated products meet ASTM D7566 specifications for ethanol-to-jet blendstock, and with energy density increases of 1.5% and 4.8%, respectively, compared to a petroleum jet fuel baseline. Furthermore, both routes offer the potential for reduced hydrogen requirements compared to more established acyclic alkane pathways. While further process optimizations are necessary to improve carbon efficiency and economic feasibility, these results highlight the potential for synthetic jet blendstocks to surpass conventional petroleum fuels in energy density. Additionally, these blendstocks demonstrate favorable O-ring swelling characteristics, complementing existing ASTM D7566 synthetic paraffinic (SPK) pathways. Moreover, their higher smoke point compared to conventional jet fuel suggests improved combustion quality and reduced particulate emissions.

Received 30th July 2025,
Accepted 1st November 2025

DOI: 10.1039/d5gc03955j

rsc.li/greenchem

Green foundation

1. This study introduces two alternative pathways for producing synthetic aviation fuel (SAF) with enhanced energy density from renewable feedstocks, strengthening the case for SAF adoption.
2. The ethanol-derived butene conversion routes produce jet-range hydrocarbons enriched in monocyclic alkanes or mixtures of mono- and bi-cyclic alkanes, achieving energy densities 1.5% and 4.8% higher than a petroleum-based jet fuel baseline. These pathways also require less hydrogen compared to conventional ethanol-to-SAF processes that yield acyclic alkanes. Additionally, the resulting liquid products meet ASTM D7566 specifications for SPK blendstocks, exhibit favorable O-ring seal swelling characteristics, support compatibility with existing jet fuel blending pathways, and offer improved combustion quality with lower particulate emissions.
3. Further catalyst and process development of the aromatization and hydroalkylation steps could reduce feedstock losses as light alkanes, enhancing carbon efficiency and overall process economics.

[a]Energy and Environment Directorate, Pacific Northwest National Laboratory, 902 Battelle Blvd, Richland, WA 99354, USA. E-mail: robert.dagle@pnnl.gov
[b]Bioproduct, Sciences, and Engineering Laboratory, School of Engineering and Applied Science, Washington State University, Richland, WA 99354, USA
[c]School of Engineering Technology, Purdue University, 401 N. Grant Street, West Lafayette, IN 47907, USA
[d]Department of Chemistry, Purdue University, 560 Oval Dr, West Lafayette, IN 47907, USA
[e]Downstream Technology Commercialization, LanzaTech, 8045 Lamon Avenue, Skokie, IL 60077, USA

1. Introduction

Synthetic aviation fuels (SAF), derived from renewable biomass and waste materials, have the potential to significantly reduce the carbon footprint compared to traditional jet fuel. These fuels provide airlines with an effective solution for cutting emissions from air travel. The use of SAF also includes benefits beyond just lower emission.[1] For example, SAF developed from a wide dispersion and variety of biomass and waste resources will ensure

that the benefits of expanded biomass production extend to both rural and urban areas. Resources, like energy crops, in a future mature market can provide more than 400 million tons of biomass per year above current uses.[2] In addition, expanding biomass production can create new economic opportunities in agriculture and urban communities, improve the environment, and even boost aircraft performance.[1]

Conventional jet fuel is composed of four primary hydrocarbon families: *n*-alkanes, iso-alkanes, cycloalkanes, and aromatics. Other molecular families, such as olefins and heteroatoms, are present only in trace amounts. High energy content is a key attribute for jet fuel, like octane in gasoline and cetane in diesel. Blending cycloalkanes and iso-alkanes can achieve greater energy content compared to jet A fuel, while still meeting the ASTM density specifications.[3] Fig. 1 illustrates how each hydrocarbon class contributes to energy content, including energy density (MJ L^{-1}) and specific energy (MJ kg^{-1}). The average composition of jet A is depicted with aromatics in yellow, monocyclic cycloalkanes in brown, bicyclic cycloalkanes in pink, *n*-alkanes in orange, and iso-alkanes in green.[3] As a mixture, the combined energy density and specific energy are represented in red, with the red hexagon indicating the average values for jet A. Note that jet A contains small amounts of multicyclic aromatics, which are not shown in the figure.[3]

The use of synthetic aviation fuel (SAF) offers the potential to improve jet fuel performance compared to conventional petroleum-based fuels. Aromatics, for instance, are harder to burn cleanly and are precursors to contrails, which amplify environmental impacts.[1] Additionally, aromatics have lower specific energy, making them less advantageous for mission performance. *n*-Alkanes also exhibit suboptimal jet fuel properties. No *n*-alkane fully meets the ASTM D1655 specifications for jet fuel—larger *n*-alkanes have high freeze points, while smaller *n*-alkanes fail to meet the flash point. While they are a readily available blending source, often derived from fatty acids and esters, *n*-alkanes as a class do not offer unique performance advantages and are not essential for SAF. Currently, SAF and renewable diesel derived from lipids are rich in *n*-alkanes.[3] Considering these factors, there are strong reasons to use SAF compositions with reduced aromatic and *n*-alkane content.[1]

From a bulk-property standpoint, jet fuel requires only iso-alkanes and cycloalkanes to meet ASTM D1655 standards. Including cycloalkanes (both mono- and bicyclic) and iso-alkanes in jet fuel formulations could enhance energy density and specific energy, satisfy freeze point and flash point requirements, support O-ring swelling, and achieve cleaner combustion.[1,3] Some studies indicate that small amounts of aromatics, preferably lightly substituted C8–C9 aromatics, may still be necessary to ensure O-ring seal swelling for backward compatibility. However, fused-ring cycloalkanes have also been suggested as an alternative, potentially providing similar seal swelling properties, along with higher energy density and cleaner combustion compared to aromatics.[3]

Iso-alkanes are particularly valued for their fuel properties but are expensive, making cost reduction a key research focus. Cycloalkanes also possess excellent characteristics, though further research is needed to address challenges such as freeze point issues or high production costs. Recent efforts aim to better understand combustion and molecular priorities, as well as production economics. For instance, recent studies have demonstrated how blending specific cycloalkanes with conventional jet fuel influences energy content, density, and viscosity.[4] However, more insights are required to fully understand how complex mixtures of iso-alkanes and cycloalkanes, produced through commercially viable pathways, affect blend properties.

PNNL and LanzaTech have developed a sustainable, non-petroleum method to produce iso-alkanes.[3,5] This process involves converting ethanol into jet fuel by first dehydrating ethanol to ethylene, followed by multi-step oligomerization.[6] Here, we present two new variations of this process that was demonstrated at the bench scale. Rather than exclusively converting the iso-olefin intermediate into iso-alkanes, these approaches utilize alternative catalytic pathways to generate mixtures of (i) mono-cycloalkanes or (ii) bicycloalkanes along with iso-alkanes. The addition of these cyclic components offers the opportunity to increase the energy density and/or specific energy of the resulting jet blendstock. Here we outline the processing steps for both pathways from ethanol, report the performance of each catalytic stage, provide ASTM fuel properties for the resulting jet-range liquids, including their energy density and specific energy, and provide preliminary understanding for how they may affect O-ring seal swelling compared to current jet fuels and blendstock.

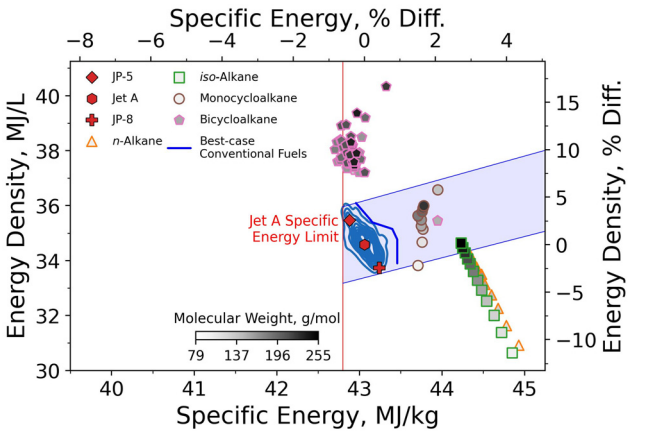

Fig. 1 Energy density and specific energy of various fuels and hydrocarbons. The red symbols depict conventional jet fuel densities taken from the Petroleum Quality Information System database. The dark blue line represents the highest value obtained from this database. Neat hydrocarbons are also plotted for reference (ref. 3).

2. Experimental

2.1 Catalyst preparation

Commercial ZSM-5 (CBV 2314, SiO_2/Al_2O_3 = 23; excluding Al_2O_3 from binder) was received in an extrudate form from

Zeolyst. The extrudates were first dried at 110 °C for 2 hours followed by calcination at 500 °C for 4 hours in stagnant air and were then ground and sieved to achieve particles smaller than 20 mesh (841 μm). The catalyst was then prepared by incipient wetness impregnation of $Zn(NO_3)_2$ solution, followed by drying under stagnant air at 110 °C for 8 hours and finally calcining under stagnant air at 400 °C for 3 hours using a 5 °C min^{-1} ramp rate. The finished catalyst was then pelletized using a die and hydraulic press and sieved to 60–100 mesh particles before loading into the reactor. Commercial SPA catalyst (Polymax 1000) extrudates were received from Clariant were crushed and sieved to 60–100 mesh particles and used without any further changes. Commercial zeolite beta powder (CP814E, SiO_2/Al_2O_3 = 25) from Zeolyst was dried at 110 °C for 2 hours followed by calcination at 500 °C for 4 hours in stagnant air. The catalyst was synthesized by incipient wetness impregnation of $Pd(NO_3)_2$ solution followed by drying under stagnant air at 110 °C for 8 hours and finally calcining under stagnant air at 500 °C for 3 hours using a 5 °C min^{-1} ramp rate. Commercial NI 5300 E nickel hydrotreatment catalyst was received from BASF in a CO_2-stabilized extrudate form and was used without further changes.

2.2 Catalyst characterization

Total acid sites were quantified using ammonia temperature-programmed desorption (NH_3-TPD) on an Autochem II 2920 Chemisorption Analyzer equipped with a thermal conductivity detector. Approximately 100 mg of catalyst was loaded into a quartz U-tube, pretreated and reduced at 400 °C for 3 hours, then saturated with 10% ammonia in helium at 100 °C. Desorption was carried out by flowing helium from 40 °C to 800 °C at a ramp rate of 5 °C min^{-1}.

X-ray diffraction (XRD) patterns were collected using a Rigaku SmartLab SE diffractometer with a copper anode ($K\alpha_1$ = 1.54059 nm), scanned from 2θ = 2° to 100° at 0.01° intervals and 3.5° min^{-1}.

Brunauer–Emmett–Teller (BET) surface areas were measured *via* nitrogen adsorption at 77 K using a Quantachrome QuadraWin analyzer. Samples were degassed under vacuum at 150 °C for 12 hours. Surface areas were calculated using the Brunauer–Emmett–Teller method over P/P_0 = 0.05–0.2, and pore size distributions were determined using the Barrett–Joyner–Halenda method.

Catalyst properties are presented in Table S1 for all the catalysts made in-house, including the 1.5% Zn/ZSM-5 before and after hydrothermal treatment and the 0.15% Pd/beta after *ex situ* reduction under 200 sccm of 5% H_2/N_2 in a tube furnace at 300 °C for 3 hours. Plots of BET adsorption–desorption isotherms, NH_3-TPD profiles, and XRD diffractograms are provided in Fig. S1, S2, and S3, respectively.

2.3 Catalyst performance testing

2.3.1 Butene aromatization. The aromatization of 1-butene was conducted in a flow-through stainless steel reactor (3/8″ diameter) equipped with a downstream liquid trap for product collection. The reactor was wrapped with heat tape, and a thermocouple placed at the center of the catalyst bed regulated the temperature. For the standard test protocol, 2.0 g of 1.5% Zn/ZSM-5 catalyst was positioned at the center of the reactor tube, secured by quartz and stainless-steel wool at both ends. A 1″ steel wool plug was placed at the top of the heated zone to facilitate the vaporization of liquid feeds. Water was introduced *via* an HPLC pump, while an ISCO syringe pump delivered 1-butene. Brooks mass flow controllers regulated the flow of gaseous hydrogen (H_2) and nitrogen (N_2).

Before performance evaluation, the catalyst underwent hydrothermal treatment *in situ*. It was heated from ambient temperature to 650 °C at a rate of 5 °C min^{-1} under atmospheric pressure with 50 sccm N_2 and 274 sccm H_2O vapor (or 0.220 mL min^{-1} liquid water) for six hours. Afterward, the water feed was discontinued, and the catalyst was cooled to the reaction temperature under a N_2 flow. A back-pressure regulator then adjusted the reactor to the desired operating pressure.

Catalytic performance was assessed under two distinct process conditions. Under conventional zeolite processing conditions, the catalyst was tested at 340 °C, 350 psig, and 0.2 h^{-1} weight-hour-space velocity for 1-butene ($WHSV_{1\text{-butene}}$). Using the "Alpha Process" conditions, testing was conducted at 515 °C, 75 psig, and 2.8 h^{-1} $WHSV_{1\text{-butene}}$. The feed consisted of a 1 : 1 molar ratio of 1-butene and nitrogen. Separate from catalyst testing, larger quantities of butene aromatization feed were produced to finally produce larger quantities of finished SAF products for fuel properties testing. For this campaign, larger catalyst loadings of 20 grams were, as well as longer times on stream of several weeks. At these time scales, deactivation by coking became a limiting issue, and the catalyst would need to be regenerated by oxidation at 515 °C under 5% O_2/N_2 for ~four hours or until no carbon oxides were detected with the on-line Micro GC; regeneration was necessary every 4–5 days.

Gas samples were periodically analyzed using an on-line 4-column Inficon Micro GC Fusion. For the aromatics alkylation with 1-butene experiments, gas samples were taken with a Shimadzu GC 2014 equipped with a RT-Q-Bond column (30 m × 0.53 mm × 20 μm film thickness) with a nitrogen carrier gas flow rate of 2.2 mL min^{-1}; this was due to the effluent gas flow rate being inadequate for the Micro GC Fusion. Liquid samples were withdrawn from the trap and examined offline *via* GC-MS using an Agilent 5795C system, equipped with an Agilent HP-5MSZ column (30 m × 0.25 mm × 0.25 μm film thickness) with helium carrier gas at a flow rate of 0.8 mL min^{-1}. The moles of aromatic compounds in the feed were estimated based on GC-MS data.

GC data was calibrated to enable semi-quantitative analysis. Peak areas were normalized to the analyzed chromatographic region, representing 95% of the total area, and converted to mass percent. While GC-MS is not inherently quantitative for complex hydrocarbon mixtures like aviation fuels, GC-FID—typically used for quantification—requires species-specific calibration, which is impractical for alcohol-to-jet products.

To validate GC-MS as a semi-quantitative tool, we examined response factors across hydrocarbon classes using a mixture of 11 model compounds in 34.5 wt% *n*-hexadecane (see

Table S5). This solution was serially diluted (2× to 100×) and analyzed using our standard GC-MS protocol. Linear regression models (Fig. S4) showed that linear olefins, paraffins, and two cycloparaffins had response factors near unity up to 3 wt%. Aromatics and bicycloalkanes exhibited higher response factors (~1.2–1.25), indicating ~20% overestimation.

Given the modest error and the low concentrations (<10 wt%) of individual species in our complex fuel mixtures, we believe GC-MS provides an accurate semi-quantitative method for this proof-of-concept study. Carbon balances for the aromatization data is shown in Fig. S5. Carbon balances measured for the alkylation runs are all within 20%.

2.3.2. Aromatics alkylation with 1-butene. In a standard 1-butene alkylation experiment, 3.0 g of SPA catalyst was loaded into the reactor, following a procedure like that used for butene aromatization. The flow reactor was equipped with tandem syringe pumps to simultaneously introduce 1-butene and the gasoline-range aromatic product from butene aromatization. The catalyst was initially heated to 200 °C under 50 sccm of N_2 at 550 psig and maintained at this temperature for two hours. Subsequently, the reactor was ramped to the reaction temperature of 220 °C, the N_2 co-feed was reduced to 4.3 sccm, and the feeds of 1-butene and aromatics were initiated. $WHSV_{1\text{-butene}}$ was set at 0.5 h^{-1}, while the WHSV for the aromatic feed ($WHSV_{aromatic}$) was approximately 0.93 h^{-1}. These space velocities were selected to achieve a 1 : 1 molar ratio between butene and aromatics.

2.3.3. Aromatics hydroalkylation. In a standard hydroalkylation experiment, 1.5 g of 0.15% Pd/BEA catalyst was loaded into the reactor following a procedure similar to that used for butene aromatization, with identical product analysis methods. The reactor was initially heated to 300 °C under a flow of 50 sccm N_2. Subsequently, the feed was switched to 120 sccm H_2, the reactor was pressurized to 270 psig, and the catalyst was maintained under these conditions for three hours to facilitate pre-reduction. After pre-reduction, the reactor was cooled to the reaction temperature of 140 °C. The $WHSV_{aromatic}$ was maintained between 1 and 2 h^{-1}, while the H_2 co-feed was adjusted to ensure a 1 : 1 molar ratio between hydrogen and aromatics.

2.3.4. Jet-range aromatics selective hydrotreatment. For the selective hydrotreatment of finished high-aromatic jet-range hydrocarbons, 54.5 g of BASF Ni 5300 E catalyst was loaded into a 1-inch diameter stainless steel reactor. The catalyst was initially dried under a N_2 flow of 1 SLPM at 180 °C for two hours, followed by reduction under 1 SLPM of H_2 at 200 °C for four hours. After reduction, the reactor was cooled to the reaction temperature of 180 °C, and the H_2 pressure was increased to 700 psig at a flow rate of 1 SLPM. The aromatic feed was then introduced, maintaining a WHSV of 1 h^{-1}.

2.4 Fuel property analysis

The jet-range hydrocarbon was analyzed using the standard tier alpha and tier beta prescreening methodology described by Heyne *et al.*[7] Tier alpha focuses on bulk composition and the distillation curve, while tier beta evaluates fuel properties relevant to combustor operability limits. Hydrocarbon-type analysis was conducted using two-dimensional gas chromatography with flame ionization detection (GC × GC-FID). The analytical methods applied are consistent with those reported in the literature.[8] Subsequent tier beta testing was performed on the jet-range hydrocarbon to assess its safety and performance characteristics. Table 1 summarizes the measured properties, corresponding instruments, and associated ASTM methods.

3. Results and discussion

Two catalytic pathways are presented for synthesizing jet-range cycloalkanes from 1-butene, an intermediate olefin commonly formed in the alcohol-to-jet (ATJ) process currently being commercialized by LanzaJet.[3] Additionally, recent literature[10,11] reports the direct production of *n*-butene-rich olefins from ethanol.[10] Instead of directly generating jet-range iso-alkanes, 1-butene is first converted into gasoline-range aromatics, which are subsequently upgraded to jet-range products *via* two distinct methods (see Fig. 2). Both approaches yield a jet-range cyclic-rich intermediate—comprising aromatics, cycloalkenes, and cycloalkanes—though each result in a different distribution of product constituents. In the first approach, aromatics derived from 1-butene undergo alkylation with *n*-butene, producing a monoaromatic-rich product. In the second method, hydroalkylation converts the aromatics into dual-ring cyclic compounds. The jet-range cyclics generated through both pathways are then selectively hydrotreated to

Table 1 Summary of measured properties, testing equipment, and corresponding ASTM methods (where applicable) for tier α and tier β evaluations

Property	Company/model	ASTM or other methods
Hydrocarbon type analysis	Agilent 8890 GC × GC-FID/VUV	Ref. 8
Simulated distillation	Agilent 8860 GC-FID	ASTM D2887
Surface tension	KRUSS – Force Tensiometer K20	ASTM D1331
Viscosity, density	Anton Paar – SVM 3001	ASTM D7042
Heat of combustion	IKA – C 3000	ASTM D4809
Hydrogen content	Bruker – minispec mq-one	ASTM D7171
Flash point	PAC – OptiFlash	ASTM D3828
Freezing point	PAC – Phase FPA-70Xi	ASTM D5972
O-ring volume swell	Optical dilatometry	Ref. 9

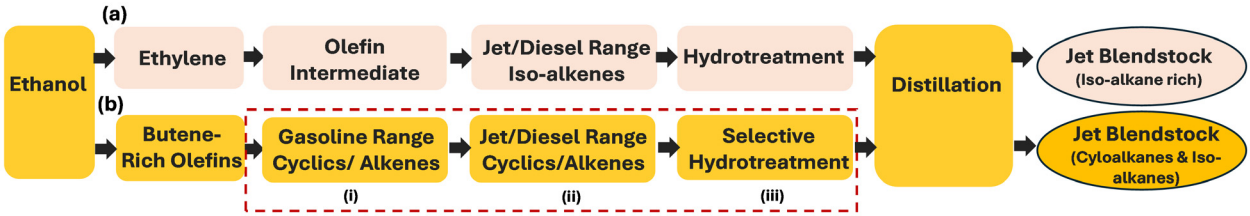

Fig. 2 Simplified process flow diagram illustrating (a) the existing LanzaJet ATJ process, which produces an iso-alkane-rich jet blendstock, and (b) the proposed process for generating a cycloalkane-rich jet fuel blendstock. The section outlined in the red box highlights the process described here, which includes three key steps: (i) aromatization of 1-butene into a gasoline-range aromatics, (ii) conversion of gasoline-range aromatics into jet-range cyclics and alkenes (*via* either butene alkylation or hydroalkylation), and (iii) selective hydrotreatment of cyclics and alkenes to produce cycloalkanes and alkanes.

produce cycloalkane-rich products. Following hydrotreatment, the liquid product is distilled to isolate a hydrocarbon fraction within the jet-range. The fuel properties of the final product can then be compared to conventional petroleum-based jet fuel and existing jet blendstocks enriched with iso-alkanes.

3.1 1-Butene aromatization (step i, Fig. 2)

The conversion of light alkanes into gasoline-range aromatics using ZSM-5 zeolite-based catalysts is well documented.[12,13] This effectiveness is attributed to the unique pore structure, shape selectivity, and acidic characteristics of ZSM-5. During aromatization, multiple reactions—including oligomerization, cracking, dehydrogenation, and cyclization—occur simultaneously over ZSM-5. To enhance product selectivity and limit side reactions such as excessive cracking, the properties of ZSM-5 are often modified by adjusting acid site distribution and introducing different active species.[13]

Beyond alkane conversion, variations of this process have been adapted for light alkenes as feedstocks.[14] This modification is necessary because light olefins, such as 1-butene, exhibit higher reactivity than alkanes due to their unsaturated double bonds. These bonds facilitate dehydrogenation and cyclization, enabling more efficient aromatization under moderate conditions. In contrast, alkanes require harsher conditions, including more energy-intensive dehydrogenation, to achieve comparable conversions.[14–18] Whether the feed for a light hydrocarbon aromatization process is olefinic or paraffinic, the overall catalyst make-up is very similar across the many variants, where a zeolitic catalyst provides acid sites to facilitate oligomerization, cracking, and cyclization and a metal species (*e.g.*, Zn, Ga, and/or Ag) provides dehydrogenation capabilities. This is common among all of the most well-known aromatization technologies, such as M2-forming,[19] Cyclar process[20] Z-forming, Aroforming, and the Alpha Process.[16] As He and coworkers wrote in their perspective on olefin aromatization for SAF production, the nature of the catalyst acid sites and dehydrogenation functionality must each be tuned for a given feedstock to provide optimum aromatics yield, low coking rate, and high H_2 co-production.[21]

A prominent example of a hydrocarbon aromatization process designed specifically for olefinic feedstocks is the Alpha Process, first reported in the literature by Sanyo Petrochemical Ltd in 1998, with a commercial plant for chemicals production in operation beginning in 1993. This process utilizes a Zn-promoted ZSM-5 catalyst that has been hydrothermally treated to reduce the external acid sites as well as strong internal acid sites, thus greatly improving catalyst stability and coking resistance. Another claim of the Alpha Process catalyst is that the hydrothermal treatment stabilizes the Zn species present in the catalyst and prevents its volatilization and loss. Additionally, the Alpha Process allows control over monoaromatic and dual-ring aromatic formation by adjusting olefin feed rates and reaction conditions. This flexibility enables the production of jet-range cyclic-rich intermediates. In contrast, acyclic alkane-based processes often yield a broader product spectrum, necessitating additional refining steps to achieve desired aromatic composition.[14,22]

First we report the conversion of 1-butene to aromatics using a 1.5% Zn/ZSM-5 catalyst reported for the Alpha Process under relatively mild temperature of 340 °C. As illustrated in Fig. 3, the liquid product comprised of 80.3% cyclics after 19 hours of time-on-stream. However, significant deactivation resulted in a reduction of the cyclic content to 59.0% after 76 hours of time-on-stream. Selectivity to gaseous hydrocarbon product decreased from 22% to 3% over the same duration. However, near complete conversion of 1-butene was observed for the entire run duration (see Fig. S5a).

It is worth noting the Alpha Process authors attributed zinc stability in their Zn/ZSM-5 catalyst to the formation of a zinc aluminate spinel, based on a model XRD study of steam-treated Zn/Al_2O_3. Their catalyst involved zinc impregnation onto ZSM-5, followed by extrusion and pelletization with an alumina binder, then hydrothermal treatment. They inferred Zn migration to the binder and spinel formation, though no XRD data was shown for the final catalyst. Our synthesis differed slightly: we used pre-pelletized ZSM-5 (already containing alumina binder), which was crushed, Zn-impregnated, and hydrothermally treated *in situ*. XRD results (Fig. S3a) show ZnO initially, and after treatment, a dominant zinc silicate phase (Zn_2SiO_3) with residual ZnO. This suggests either (1) our modified procedure prevented spinel formation, or (2) the original claim based on model ZnO/Al_2O_3 was incorrect.

The performance of this catalyst was also evaluated under the same temperature, pressure, and space velocity as indi-

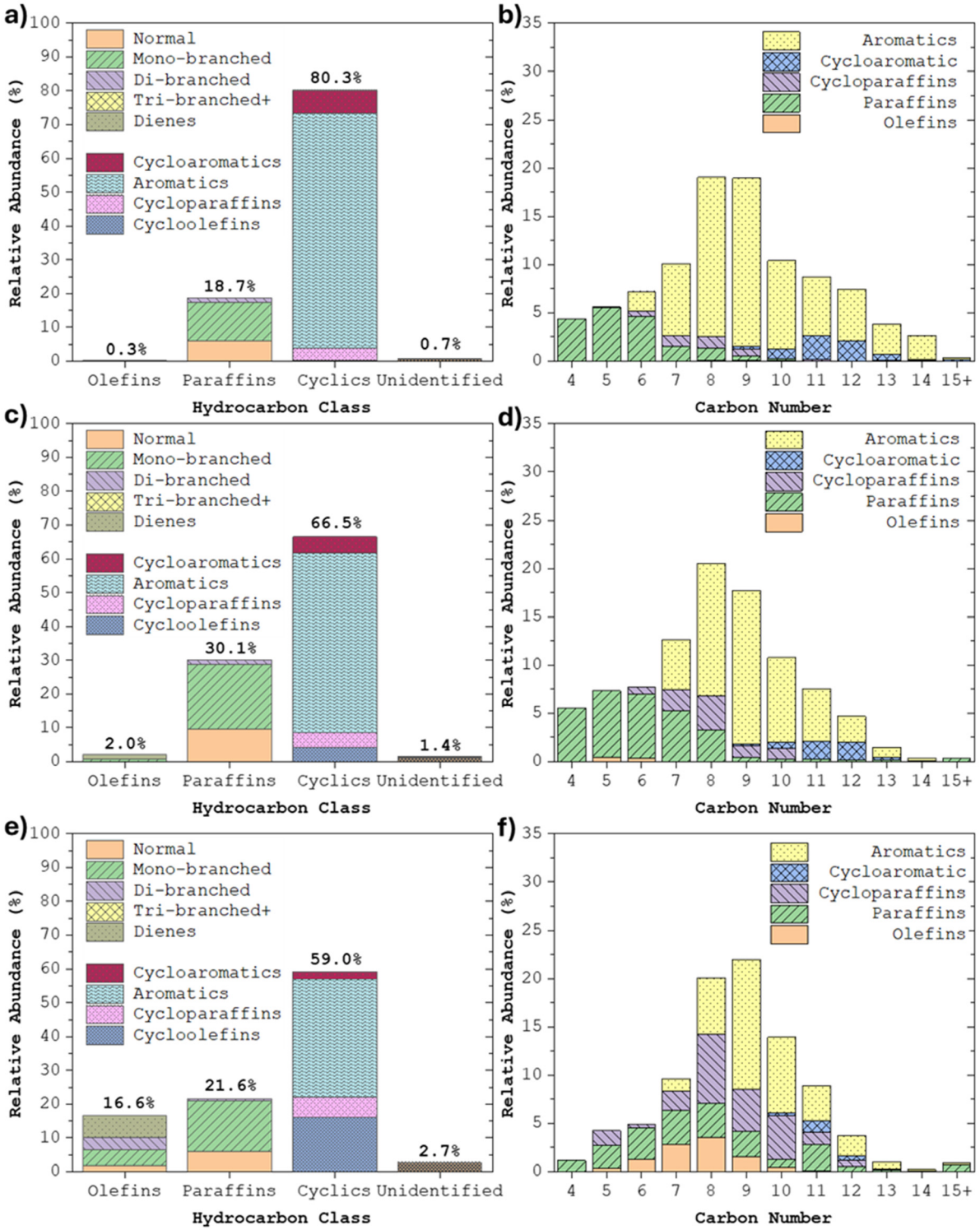

Fig. 3 Conversion of 1-butene over hydrothermally-treated 1.5%Zn/ZSM-5 (SiO_2/Al_2O_3 = 23) and resulting (a, c and e) liquid product classification and (b, d and f) carbon number distribution at (a and b) 19, (c and d) 51, and (e and f) 76 hours' time on stream (T = 340 °C, P = 350 psig, $WHSV_{1\text{-butene}}$ = 0.19 h^{-1}; feed = 50 mol% 1-butene in N_2).

cated in the original Alpha Process publication.[14] In this case, the catalyst was tested at a higher temperature (515 °C *vs.* 340 °C) and lower pressure (75 psig *vs.* 350 psig), as outlined earlier. As shown in Fig. 4, the catalyst demonstrated excellent stability over a 29-hour run, producing a 94% cyclic liquid product, primarily within the gasoline range. Notably, the

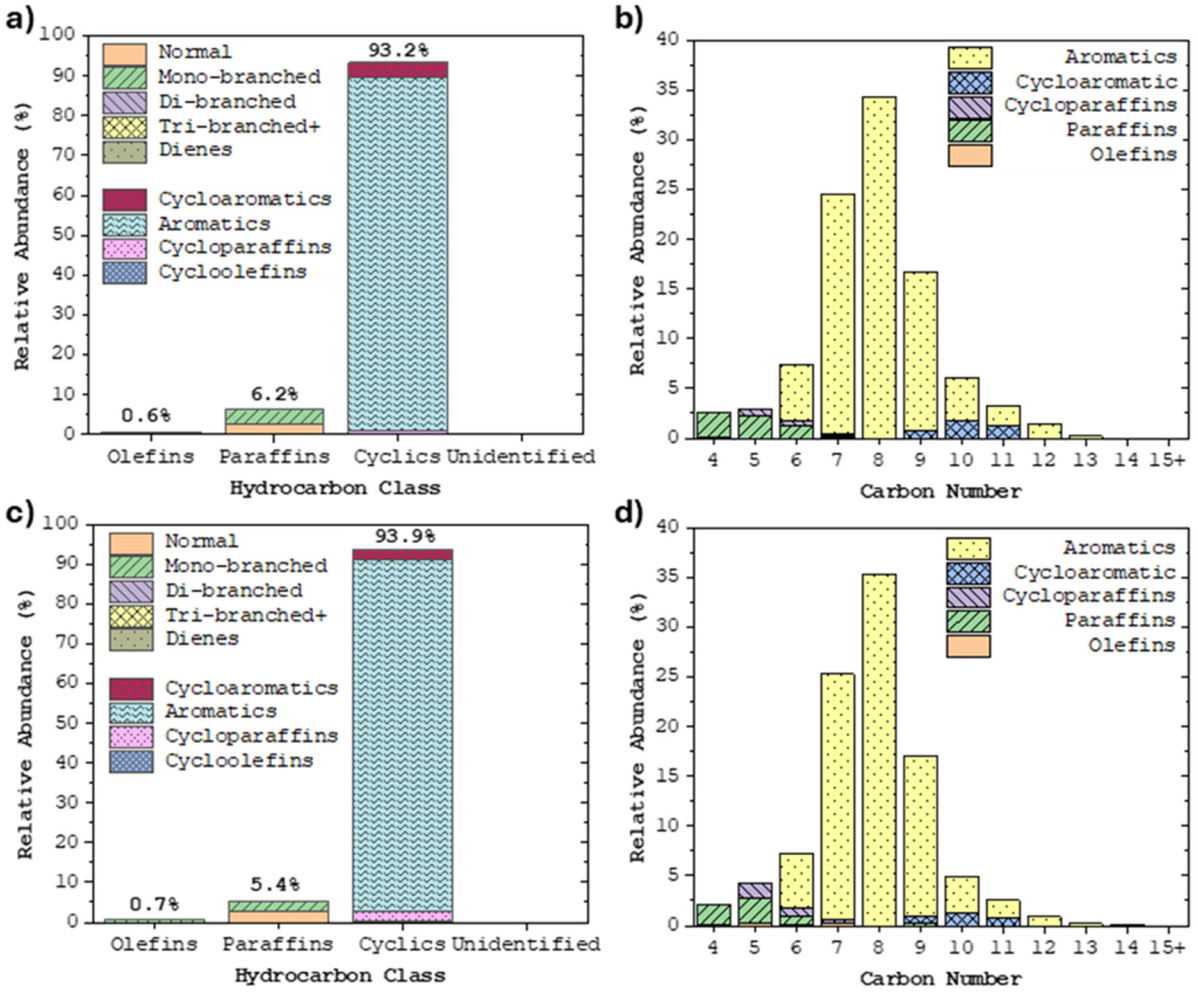

Fig. 4 Conversion of 1-butene over hydrothermally treated 1.5% Zn/ZSM-5 (SiO_2/Al_2O_3 = 23) and resulting (a and c) liquid product classification and (b and d) carbon number distribution at (a and b) 8 and (c and d) 29 hours' time-on-stream (T = 515 °C, P = 75 psig, $WHSV_{1\text{-butene}}$ = 2.8 h^{-1}).

weight hourly space velocity (WHSV) for this run was significantly higher (2.8 h^{-1}) than that in Fig. 3 (0.9 h^{-1}), enabled due to the higher temperature of operation. Consequently, despite the shorter run duration (29 hours), the total amount of 1-butene processed remained similar, owing to the higher WHSV employed.

These results confirm that the hydrothermally treated Zn-promoted ZSM-5 catalyst generated a liquid product rich in cyclics (~93%) while exhibiting markedly improved catalyst stability under higher-temperature, lower-pressure conditions. Additionally, 1-butene conversion exceeded 98% throughout the entire 8+ hour experiment. While our replication of the Alpha Process catalyst synthesis was not precisely the same as originally reported, we appear to have achieved the same overall dual outcomes of producing a stable Zn phase active for dehydrogenation and decreasing the overall acidity to reduce deactivation by coking, which can be seen in the comparison of the ammonia TPD profiles in Fig. S2. Additionally, the hydrothermal treatment, which reasonably could have acted as a zeolite dealumination procedure as well, appears to have potentially introduced some mesoporosity as seen in Table S1, where the surface area and pore size both increase after hydrothermal treatment. This fact could also be a beneficial factor in the catalyst stability, as the larger pore openings made by dealumination could allow bulky coke precursors to diffuse out of the microchannels more effectively.

To extend this proof of concept to a realistic mixture of higher olefins from an ethanol-to-jet pathway, we used a butene-rich intermediate, produced from ethylene, comprising 70% C_4, 27% C_6, and 3% C_8 acyclic olefins. This feedstock was evaluated under the same process conditions as the model butene feed and as shown in Fig. S6, exhibited comparable stability and selectivity for liquid aromatics. Notably, it produced a modest increase in C_{10+} hydrocarbon yield—an outcome that further supports the ethanol-to-cycloparaffin jet fuel pathway. This demonstrates that mixtures of butene-rich higher olefins provide a similar product slate and comparable catalyst stability as with model butene alone.

Despite notable improvements in catalyst stability, a substantial fraction of gaseous hydrocarbons (~40%) was still pro-

duced under reaction conditions (see Fig. S5b). While operating at elevated temperatures improved catalyst durability and boosted aromatic selectivity, it also promoted light alkane formation and gradual deactivation due to coking—highlighting the need for further catalyst and process optimization to enhance carbon efficiency. Coking could potentially be mitigated by adjusting catalyst acidity, such as quenching excessive acid sites through alkali metal doping.[23] Alternatively, hierarchical Zn/ZSM-5 catalysts with enlarged mesopores—achieved *via* desilication or bottom-up synthesis—have been reported to improve coke precursor diffusion, preserving selectivity and extending catalyst life.[24] To reduce light alkane formation, these byproducts could be recycled and reprocessed to improve carbon efficiency, though minimizing their generation in a single pass is preferable. Prior studies indicate that alkane formation can be suppressed by fine-tuning the dehydrogenation activity of Zn species, either by modifying Zn nuclearity (*e.g.*, promoting cationic Zn sites) or incorporating additional dehydrogenation co-catalysts to enhance aromatic yield.[25]

3.2 Conversion of gasoline- to jet-range aromatics (step ii, Fig. 2)

The next process step is designed to upgrade the product slate into the jet-range fraction. Two approaches were evaluated to achieve this. First, the cyclic-rich product from the primary gasoline-range liquid generated in step (i) (see Fig. 2) was alkylated with butene using a well-known solid phosphoric acid (SPA) alkylation catalyst.[26] As illustrated in Fig. 5, this approach significantly increased the jet fraction, nearly fourfold, rising from 15.6% to 63.5%. Table S3 presents the ten most abundant compounds identified in both the liquid product and the jet-range fraction. The liquid product primarily consists of alkyl-substituted benzene compounds, with smaller quantities of dual-ring naphthenic species also present. Since the product primarily consists of olefins and aromatics, further optimization—such as reducing the weight hourly space velocity (WHSV) or recycling fractions lighter than the jet-range—will enhance carbon distribution toward

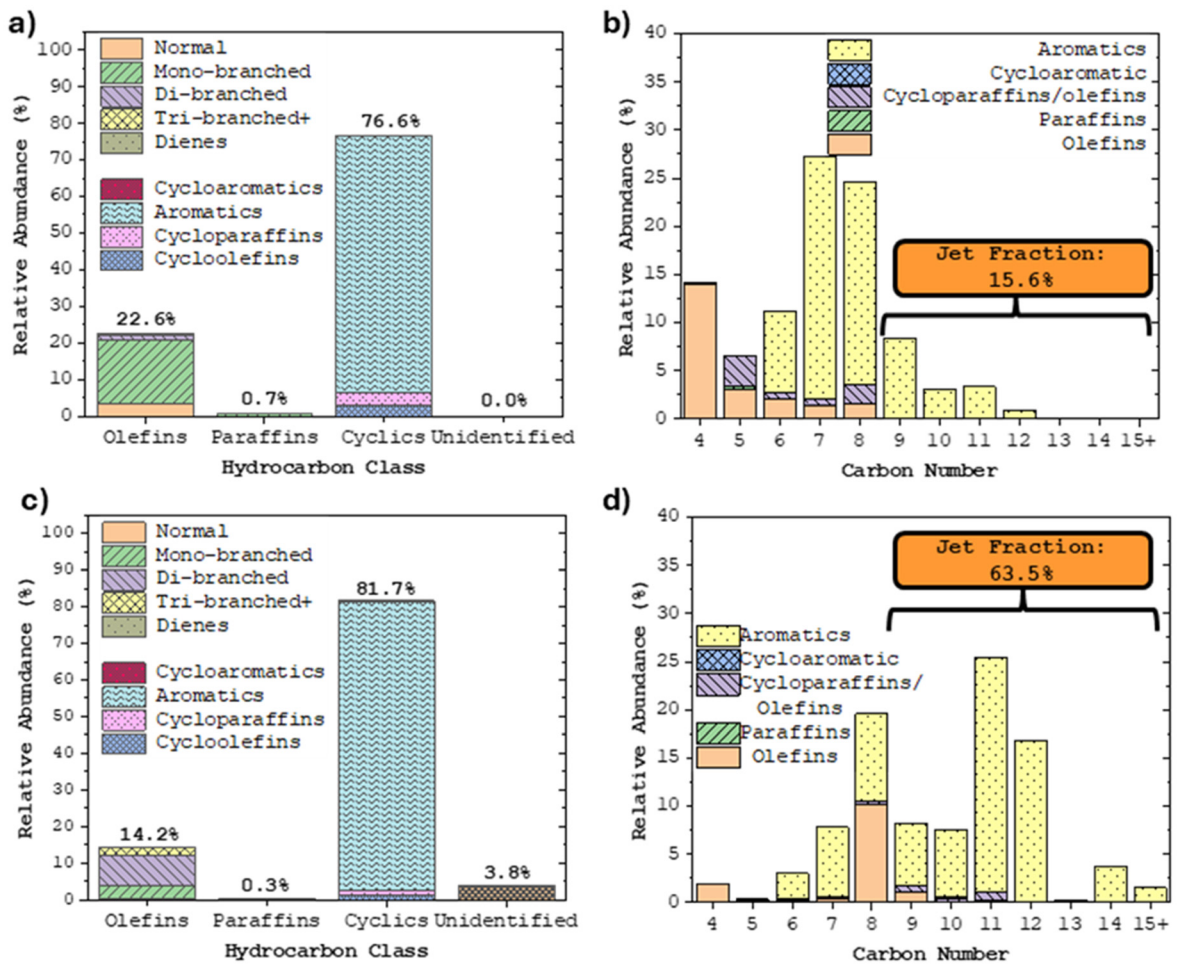

Fig. 5 (a) Liquid product classification and (b) carbon number for the high aromatic content feed (as performed in step i, Fig. 2); and resulting (c) liquid product composition and (d) carbon number distribution after alkylating this feedstock with 1-butene after 17.5 hours' time-on-stream (step ii; feed: cyclic feed/1-butene = 1/1 mol; SPA catalyst; 220 °C, 550 psig, 1.5 h^{-1} WHSV).

jet-range hydrocarbons. Additionally, the light fractions from step (i) could be integrated into the feedstock at this stage, effectively eliminating the need for recycling in step (i). Finally, we note that liquid product formation remained stable when comparing outputs at 6 and 18 hours' time-on-stream (see Fig. S7).

In the second approach for enhancing carbon number distribution, we report the hydroalkylation of aromatics. This process involves the alkylation of two cyclic rings in the presence of hydrogen and a bifunctional metal-acid catalyst. The hydroalkylation of benzene is well documented in the literature as a method for producing cyclohexylbenzene, which has applications as a solvent and plasticizer in plastics, coatings, and adhesives.[27] According to published studies, the hydroalkylation reaction pathway involves partial hydrogenation of benzene at the metal site, generating cyclohexene, which then undergoes alkylation at the acid site to form cyclohexylbenzene (see Scheme 1). It is desired to limit byproducts including dicyclohexylbenzene, cyclohexane, and bicyclohexane when producing cyclohexylbenzene.[27] However, for fuel synthesis, the formation of these intermediates and product species may be advantageous, contributing to desirable fuel properties.

While the literature documents various supports and metals for hydroalkylation, this study reports the use of a promising 0.15% Pd/BEA catalyst[28] to hydroalkylate a high-aromatic product derived from the Zn/ZSM-5 aromatization catalyst. Experimental conditions evaluated included temperatures ranging from 140 to 220 °C, pressures from 160 to 370 psig, a constant weight hourly space velocity (WHSV) of 2.0 h^{-1}, and a fixed H_2-to-aromatic molar feed ratio of 1 : 1. The optimal results were achieved at 140 °C and 270 psig, as shown in Fig. 6. The single pass increase in the jet fraction was twofold (from 18.3% to 44.0%), which, while significant, is lower than the fourfold increase observed with conventional alkylation (from 15.6% to 63.5%, as seen in Fig. 5). Table S4 lists the ten most abundant compounds found in both the liquid product and the jet-range fraction. The liquid product consists of a substantial amount of dual-ring cyclic compounds, including cycloaromatics, alongside alkyl-substituted benzene compounds, which are similar to those present in the conventional alkylated product (see Table S3). We also note that liquid product formation remained stable when comparing outputs at 2, 4, and 6 hours' time-on-stream (see Fig. S8).

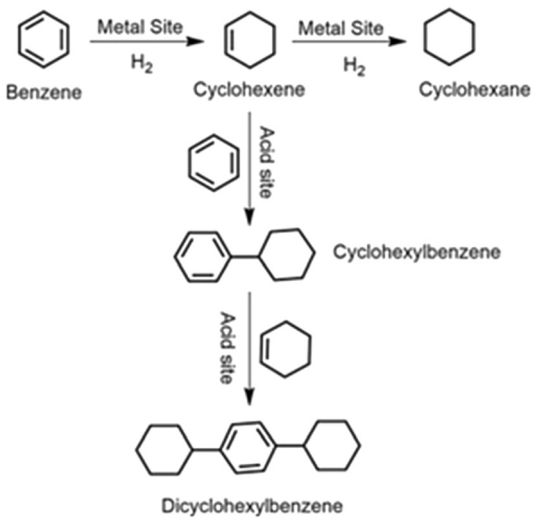

Scheme 1 Reaction mechanism shown for hydroalkylation of benzene to cycloolefin alkylates, over bifunctional catalyst comprising metal and acid sites (republished with permission from ref. 27).

With hydrogen present in the feed, hydroalkylation results in a higher proportion of alkanes (~7%, as shown in Fig. 6) compared to alkylation (<1%, as shown in Fig. 5). This includes greater fractions of C7 and C8 cycloparaffins, which present recycling challenges since they are inactive for hydroalkylation. However, these cycloparaffins could be dehydrogenated back into aromatics if recycled to the aromatization reactor used in the first step, alongside the lighter-than-jet olefins and aromatics. Hydroalkylation inherently offers challenges to selectivity control; however, further optimization of both the catalyst and process could significantly enhance carbon efficiency toward the jet-range fraction. Patent literature that inspired this application highlights a broad array of metal active sites (*e.g.*, Ni, Ru, Pd, Pt) supported on various frameworks such as Zeolite Beta, Mordenite, and MCM-22, providing a strong foundation for exploring alternative catalysts with improved conversion and selectivity.[28–30]

In this study, Pd/BEA was selected as a straightforward and accessible catalyst reported to deliver reasonable single-pass yields of hydroalkylates. Academic literature emphasizes that selectivity and conversion in such systems depend on a delicate interplay between metal and acid sites.[27,31,32] To advance this approach, future work could investigate the co-adsorption behavior of target aromatics on bimetallic formulations, zeolites with tuned acidity, and particularly mesoporous supports that facilitate diffusion of bulky intermediates like xylenes. These strategies could yield hydroalkylation catalysts better suited to this specific application, beyond conventional benzene/toluene systems.[28] Taken together, hydroalkylation remains a promising avenue for further development, especially given its energy density and hydrogen requirement advantages.

3.3 Selective hydrogenation of aromatics to cycloalkanes (step iii, Fig. 2)

In the final catalytic step, aromatic-rich cyclic mixtures undergo selective hydrotreatment to form cycloalkanes, while ensuring that undesirable side reactions, such as ring opening or cracking, are avoided. Hydrogenation of both the alkylated (Fig. 5) and hydroalkylated (Fig. 6) products was conducted using a commercial Ni-based hydrotreating catalyst. As shown in Fig. S9, the alkylated feedstock, with a cyclic content of ~81%, primarily composed of aromatics, was successfully hydrogenated into its cycloalkane analogs with no observable cracking or ring-opening side reactions. Similarly, in Fig. S10, the hydroalkylated product was converted into its cycloalkane analogs. In both cases, alkenes, cycloalkenes, and aromatics

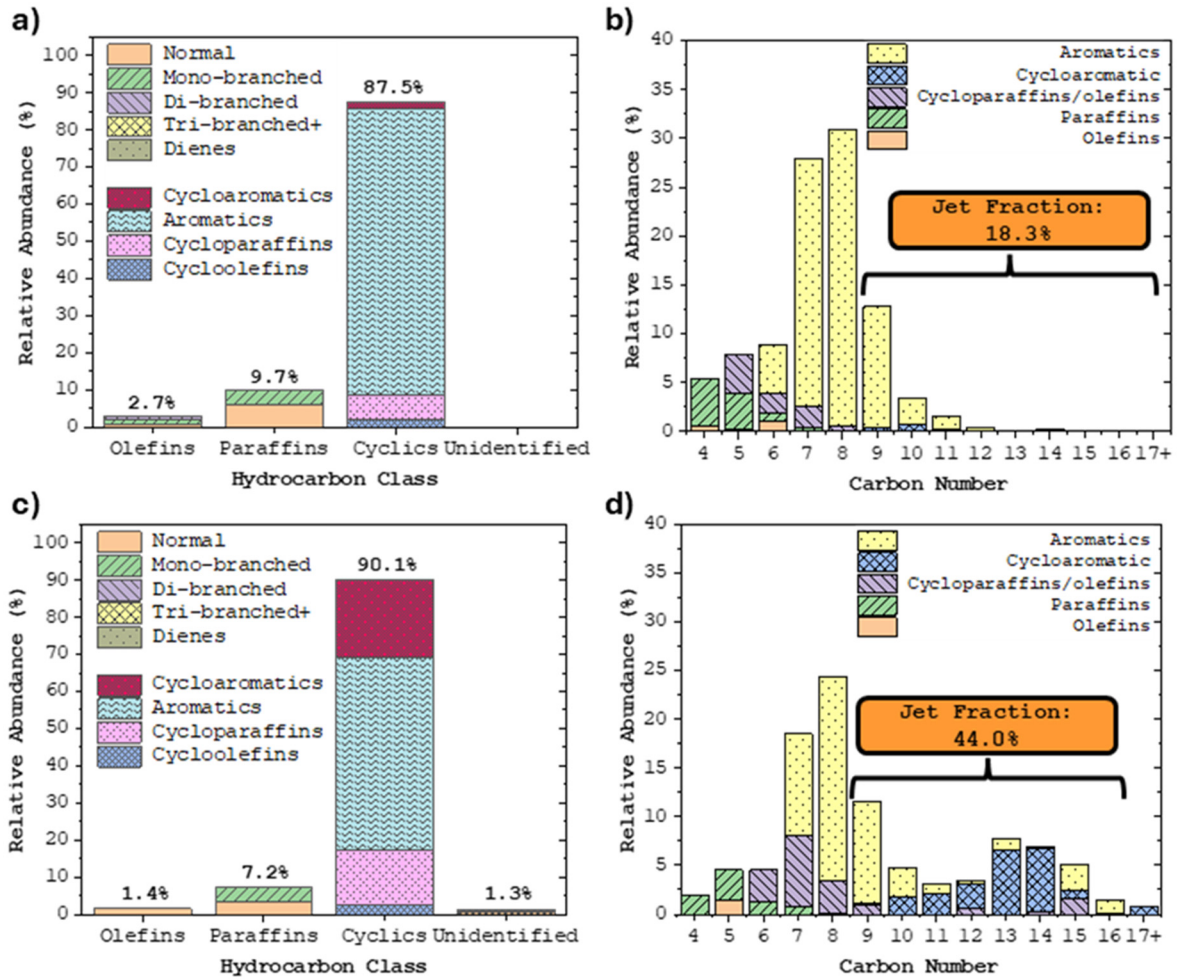

Fig. 6 (a) Liquid product classification and (b) carbon number for the high aromatic content feed (step i, Fig. 2); (c) liquid product composition and (d) carbon number distribution for the hydroalkylation product after 6 hours' time-on-stream (step i; feed: aromatic feed/H_2 = 1/1 mol; 0.15% Pd/BEA catalyst; 140 °C, 270 psig, 2.0 h^{-1} WHSV).

present in the liquid phase were effectively hydrogenated to their corresponding alkanes and cycloalkanes with over 97% conversion. It is worth noting that further optimization of process conditions could enhance saturation levels, as mature systems have demonstrated hydrogenation efficiencies exceeding 99%.

3.4 Ethanol to jet reaction pathways

This report introduces two new ethanol-to-fuel conversion pathways centered on the transformation of butene-rich olefins into gasoline-range aromatics, followed by either (i) alkylation with additional butene to form monocycloalkanes or (ii) hydroalkylation of aromatics to form bicyclic alkanes. These two approaches—illustrated in Fig. 7—represent novel alternatives to the conventional acyclic alkane pathway and expand the scope of ethanol-derived sustainable aviation fuel (SAF) production.

To contextualize these innovations, we examine the broader ethanol-to-fuel processing landscape. Across all three pathways considered here—acyclic alkanes and alkyl-substituted di- and mono-cycloalkanes—ethanol is usually first dehydrated to ethylene followed by its oligomerziaiton to butene and higher olefins.[6] Recent studies have also demonstrated the direct conversion of ethanol to butene-rich olefins,[10] offering an alternative to the conventional two-step process of ethanol dehydration followed by ethylene dimerization. In conventional ethanol-to-acyclic alkane pathways, higher olefin intermediates like butene typically undergo oligomerization to produce jet-range iso-olefins, which are subsequently hydrogenated and distilled.[6] In contrast, the alternative pathways reported here convert butene-rich olefins into aromatics that are either alkylated with butene to ultimately produce monocycloalkanes or hydroalkylated to yield alkyl-substituted mono- and dicycloalkanes, formed after hydrogenation of unsaturated carbon–carbon bonds. Table 2 presents the generalized idealized net reactions for these fuel hydrocarbon types, illustrating the differing hydrogen requirements: the acyclic alkane route requires additional hydrogen input, the monocycloalkane

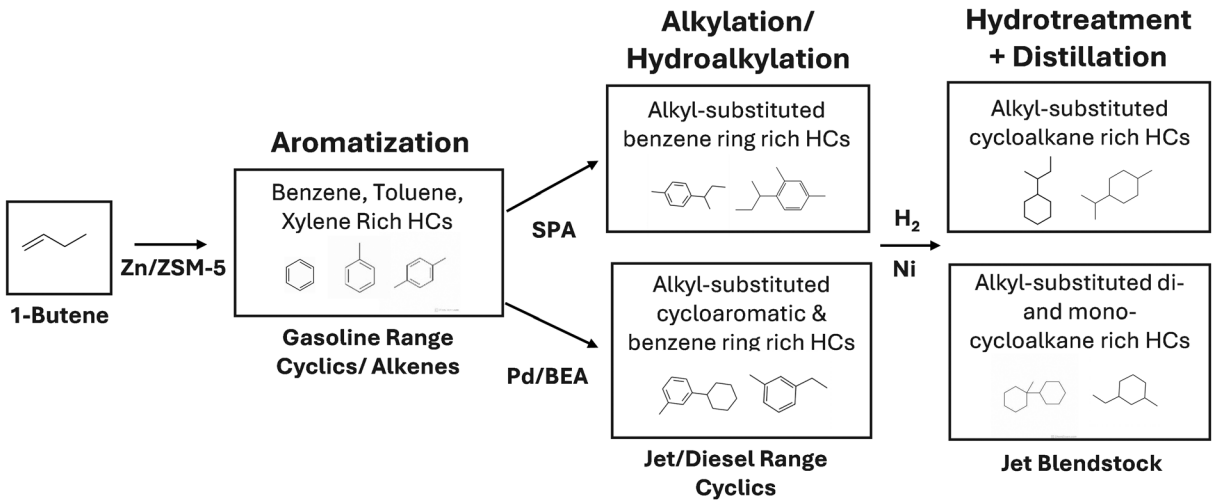

Fig. 7 Simplified process flow diagram for the two approaches reported here for converting gasoline-range aromatics into either (i) alkyl-substituted cycloalkane rich hydrocarbons (HCs) or (ii) alkyl-substituted di- and mono-cycloalkane rich HCs in the jet-range.

Table 2 Idealized net reactions and corresponding hydrogen balance for ethanol conversion to representative hydrocarbon fuel types

Target hydrocarbon type	Idealized net reaction	Net H_2 balance per fuel mole (mol)
Acyclic alkanes (C_nH_{2n+2})	$(n/2)C_2H_5OH + H_2 \rightarrow C_nH_{2n+2} + (n/2)H_2O$	+1 (H_2 required)
Single-ring cycloalkanes (C_nH_{2n})	$(n/2)C_2H_5OH \rightarrow C_nH_{2n} + (n/2)H_2O$	0 (no H_2 required or produced)
Two-ring cycloalkanes (fused or non-fused, C_nH_{2n-2})	$(n/2)C_2H_5OH \rightarrow C_nH_{2n-2} + (n/2)H_2O + H_2$	−1 (H_2 produced)

The net H_2 balance reflects the number of moles of hydrogen required or produced per mole of target fuel product, based on reaction stoichiometry.

route is hydrogen-neutral, and the dicycloalkane route yields a net hydrogen surplus. Table S5 further details the idealized reactions for each step in all three pathways, using C_{16} fuel products as representative examples.

This analysis of the idealized net reactions highlights key trade-offs in hydrogen demand and carbon utilization, providing a comparative framework for assessing process efficiency and integration potential. In practice, however, the reaction pathways are more complex, producing mixed outputs and undergoing side reactions that affect efficiency, cost, and overall performance. For context, a leading ethanol-to-jet-range iso-alkane conversion has demonstrated overall yields exceeding 85% from ethanol to jet fuel blendstocks.[6] In contrast, the alternative chemistries explored here have shown significantly lower product yields. As detailed in Table S6, both pathways – either *via* alkylation or hydroalkylation – are currently limited by the modest aromatic yield from butene (~40%). Notably, aromatic production was not optimized in this study, as it represents a mature process with higher yields reported elsewhere. Instead, our focus was on evaluating the relative benefits of butene alkylation and hydroalkylation of aromatic intermediates. Carbon yields for the key steps—butene alkylation of aromatics, hydroalkylation, and hydrogenation—were approximately 92%, 76%, and 97%, respectively (see Table S6). Collectively, these findings highlight the need for significant advancements—especially in aromatization and hydroalkylation—to enhance competitiveness with conventional acyclic alkane-based processes. Given that ethanol feedstock cost is a major factor in process economics, maximizing carbon yield is essential for achieving commercially viable performance.

3.5 Fuel properties of jet-range hydrocarbons

To evaluate the fuel properties of the hydrocarbons produced in this study, the hydrotreated cycloalkane-rich products were subsequently fractionated to isolate the jet-range fraction. For the alkylated product, 61.4 wt% of the liquid product fell within the jet range (see Fig. S9). In contrast, the hydroalkylated product yielded only 32.7% within the jet range (see Fig. S10). We note that further process optimization, such as recycling the lighter-than-jet-range hydrocarbons, as discussed above, is needed to increase carbon efficiency to the jet-range. However, the primary goal of this study is to evaluate how these fuel blends impact jet-range fuel properties to determine whether further process refinements are warranted.

The jet-range hydrotreated samples were thus assessed for safety compliance and performance characteristics. The alkylated product exhibited a carbon number and distillation profile consistent with average conventional jet fuel, though skewed toward the lower end of the range (see Fig. 8). Importantly, all properties that are described in ASTM D7566 specifications were successfully met for the ethanol-to-jet blendstock. Those properties are surface tension [σ (22 °C)],

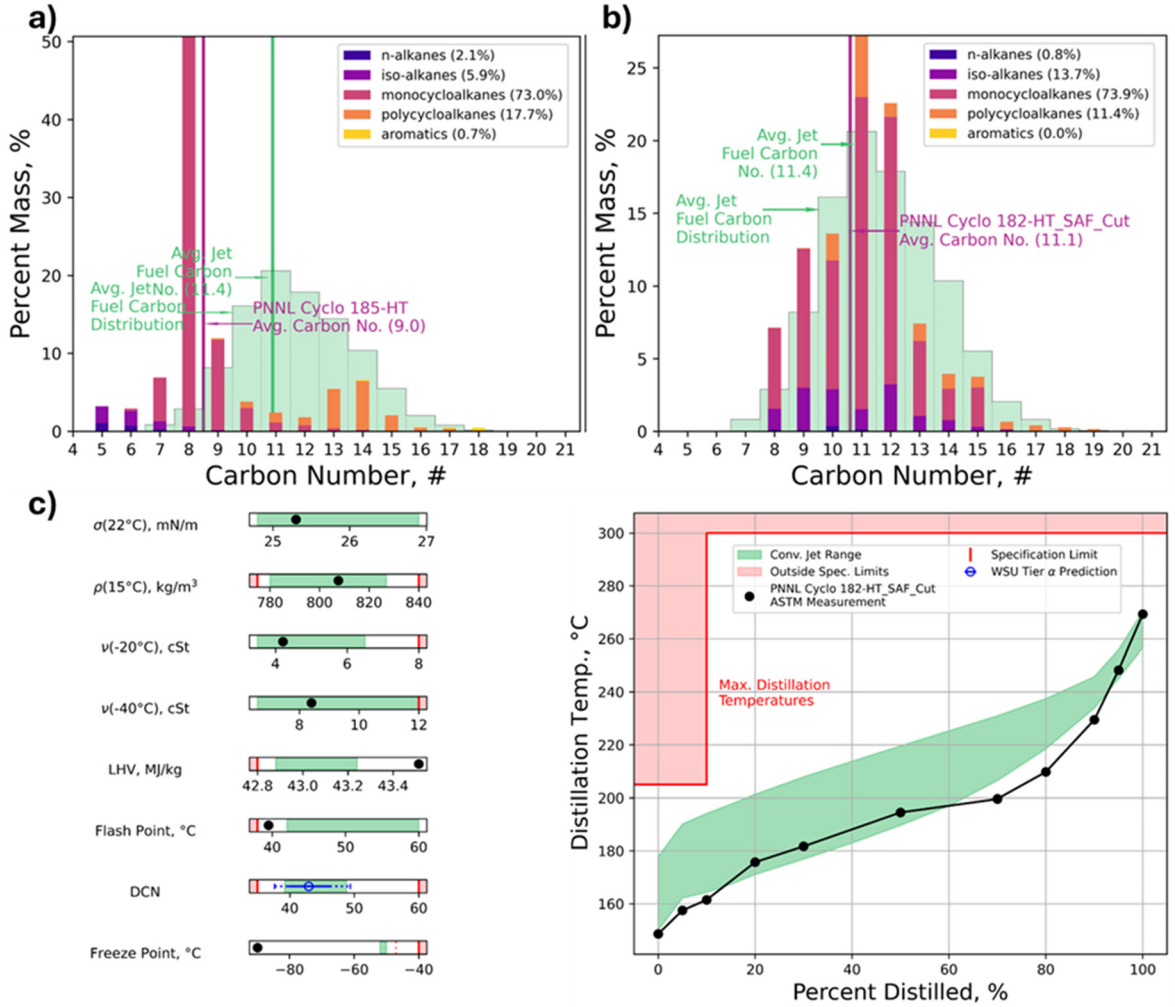

Fig. 8 (a) Full distillate sample of the alkylated product after hydrotreatment (see Fig. S6d). (b) Jet range (>130 °C b.p. cut) after distillation. The green shaded region represents the carbon distribution of an average conventional jet fuel for reference. (c) Tier beta property measurement for the jet range hydrocarbons.

density [ρ (15 °C)], viscosity [ν (−20, −40 °C)], lower heating value (LHV), flash point (°C), derived cetane number (DCN), and freeze point (°C). The green shaded regions represent the conventional jet fuel experience range, while the red bars and red shaded regions indicate specification limits and values outside the specification limit as defined by ASTM D1655 and D7566. Similarly, for the hydroalkylated product, its carbon number and distillation profile differed, likely due to its bimodal carbon number distribution. However, it also met ASTM standards (see Fig. 9).

An important finding from this study pertains to the energy content of the produced jet blendstocks. As shown in Table 3, incorporating cycloalkanes into iso-alkanes resulted in a slight reduction in specific energy density for both the alkylated and hydroalkylated products. However, compared to conventional jet fuel, the specific energy of the alkylated product was 1.1% higher, while the hydroalkylated product exhibited a negligible decrease (−0.1%). Notably, the addition of cycloalkanes significantly increased energy density, with the alkylated product showing a 1.5% rise and the hydroalkylated product demonstrating an even greater increase of 4.8%. These enhancements highlight the potential of cycloalkanes in improving overall fuel performance.

Both specific energy and energy density are important considerations for jet fuels, with their importance varying depending on the application. Specific energy (energy per unit mass) is relevant for aircraft performance as it directly affects fuel weight. Higher specific energy reduces fuel weight, leading to improved efficiency and increased payload capacity. On the other hand, energy density (energy per unit volume) is important for fuel storage and tank design. Greater energy density allows more energy to be packed into a smaller space, benefiting aircraft with limited storage capacity.[33,34] For commercial aviation, both factors are important, but energy density is often prioritized to maximize storage capacity. For military and high-performance aircraft, specific energy is critical for maneuverability, efficiency, and combat range.[33,34] Importantly, the flexibility to customize synthetic aviation

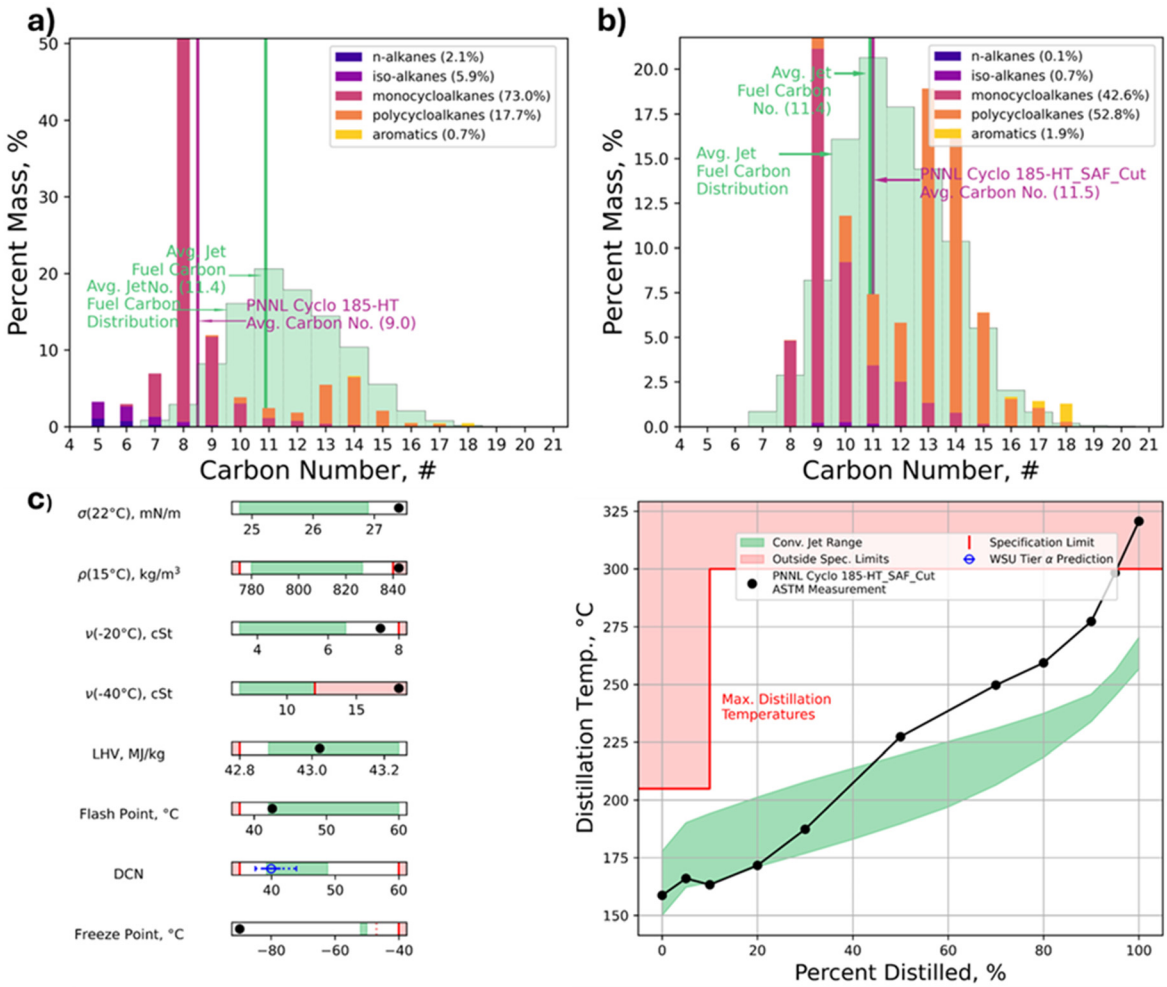

Fig. 9 (a) Full distillate sample of the alkylated product after hydrotreatment (see Fig. S7d). (b) Jet range (>130 °C b.p. cut) after distillation. The green shaded region represents the carbon distribution of an average conventional jet fuel for reference. (c) Tier beta property measurement for the jet range hydrocarbons.

Table 3 Energy density and specific energy comparisons between jet A, and LanzaTech and alkylated and hydroalkylated liquid products after hydrotreatment and distillation

				Percent difference *versus* jet A (%)	
		Specific energy, MJ kg^{-1}	Energy density, MJ L^{-1}	Specific energy, MJ kg^{-1}	Energy density, MJ L^{-1}
Unblended	Jet A	43.06	34.58	n/a	n/a
Blendstock	Iso-alkanes (*e.g.*, LanzaJet)	43.90	33.50	2.0	−3.1
	Mono-cycloalkane-rich	43.51	35.11	1.1	1.5
	Bicycloalkane-rich	43.02	36.24	−0.1	4.8

fuels with different blends allows for tailoring properties to suit specific applications and needs.

3.6 O-ring and emission properties of jet-range hydrocarbon products

Additional materials compatibility and combustion/emission characteristics were also evaluated for the jet-range hydrocarbon products. Fig. 10 shows the relationship between O-ring volume swell and aromatic content. Both products exhibited favorable volume swell behavior with only minimal aromatic content (<3%), which is consistent with the performance of fuels rich in cycloalkanes.[35] The combination of high swelling potential and elevated density makes this product a strong complement to existing ASTM D7566 synthetic paraffinic kerosene (SPK) pathways, which primarily yield *n*- and iso-alkanes.

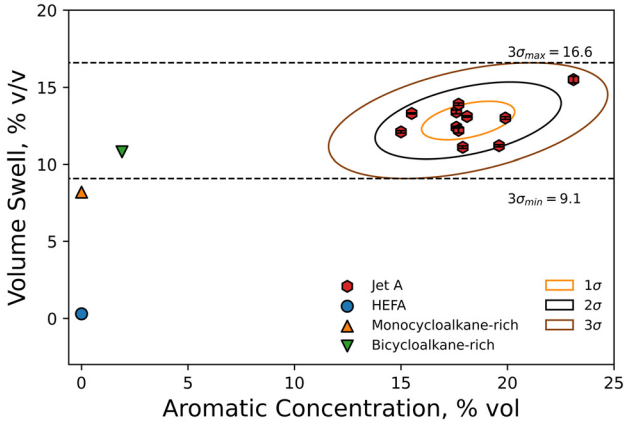

Fig. 10 O-ring volume swell verse aromatics concentration of both mono-cycloalkane-rich and bicycloalkane-rich blendstocks.

Emission characteristics were also assessed. Both samples demonstrated smoke point values of 31.8 mm for the monocycloalkanes-rich product and 27.0 mm for the bicycloalkanes-rich product, higher than the average smoke point of approximately 25 mm for conventional jet fuels. These elevated smoke point values suggest improved combustion quality and reduced particulate emissions.

4. Conclusion

This proof-of-concept bench-scale demonstration introduces two catalytic pathways for producing cycloalkane-rich liquid products from ethanol. Both approaches utilize a butene intermediate that can be derived from the existing LanzaTech/LanzaJet alcohol-to-jet process or produced directly from ethanol. The new processes reported here involves three key steps: (i) aromatization of the butene intermediate into gasoline-range aromatics, (ii) increasing the carbon distribution from gasoline to jet-range cycloalkanes *via* alkylation or hydroalkylation, and (iii) selective hydrogenation of cyclic intermediates—including cycloaromatics, aromatics, cycloalkanes, and cycloolefins—resulting predominantly in cycloalkane mixtures. Olefins present in the feed are also primarily hydrogenated into corresponding alkanes.

The alkylation route primarily yields jet-range monocycloalkanes, while the hydroalkylation pathway produces mixtures of mono- and bicyclic alkanes, offering enhanced energy density. Both pathways also present the potential for reduced hydrogen requirements compared to SAF processes that generate acyclic alkanes. However, further optimization is needed to improve carbon efficiency and ensure economic viability for commercialization. This study demonstrates that ethanol-derived iso-alkane and cycloalkane mixtures can produce SAF that meets ASTM fuel property standards and delivers superior energy density relative to conventional petroleum-based jet fuel. Further, being low in aromatic content (<3%), these blendstocks exhibit favorable O-ring swelling characteristics, supporting the certification and adoption of 100% unblended SAF for commercial aviation. Additionally, their higher smoke points suggest improved combustion quality and lower particulate emissions.

The alkylation route mainly produces jet-range monocycloalkanes, while the hydroalkylation pathway yields mixtures of mono- and bi-cyclic alkanes, offering energy density advantages. Both also offer the potential for reduced hydrogen requirements over SAF pathways that produce acyclic alkanes. Regardless, both routes would require optimization to achieve carbon efficiency while remaining economically viable for commercialization. Nonetheless, this study demonstrates how these mixtures of ethanol-derived iso-alkanes and cycloalkanes can produce SAF that meets ASTM fuel property standards and provides superior energy density compared to conventional petroleum-based jet fuel. Furthermore, with favorable O-ring swelling properties, these blendstocks may pave the way for the certification and adoption of 100% unblended SAF for commercial aviation. Moreover, their higher smoke point compared to conventional jet fuel suggests improved combustion quality and reduced particulate emissions.

Conflicts of interest

There are no conflicts to declare.

Data availability

The data supporting this article have been included as part of the supplementary information (SI). Supplementary information is available. See DOI: https://doi.org/10.1039/d5gc03955j.

Acknowledgements

The authors gratefully acknowledge funding for this research, provided by the U.S. Department of Energy (DOE), Office of Energy Efficiency and Renewable Energy, Bioenergy Technologies Office and performed at Pacific Northwest National Laboratory (PNNL). PNNL is a multi-program national laboratory operated by Battelle for the U.S. Department of Energy under contract DE-AC06-76RL0183. The authors extend their gratitude to Teresa Lemmon and Marie Swita for their invaluable analytical support on this project, as well as to Conor Faulhaber for his contributions to seal swell measurements.

The views and opinions of the authors expressed herein do not necessarily state or reflect those of the U.S. Government or any agency thereof. Neither the U.S. Government nor any agency thereof, nor any of their employees, makes any warranty, expressed or implied, or assumes any legal liability or responsibility for the accuracy, completeness, or usefulness of any information, apparatus, product, or process disclosed, or represents that its use would not infringe privately owned rights.

References

1 https://www.energy.gov/eere/bioenergy/synthetic-aviation-fuels, last accessed April 8, 2025.
2 https://www.energy.gov/sites/default/files/2024-03/beto-2023-billion-ton-report_2.pdf, last accessed April 8, 2025.
3 https://www.energy.gov/sites/default/files/2020/09/f78/beto-sust-aviation-fuel-sep-2020.pdf, last accessed April 8, 2025.
4 L. E. Caceres-Martinez, J. Saavedra Lopez, R. A. Dagle, R. Gillespie, H. I. Kenttämaa and G. Kilaz, Influence of blending cycloalkanes on the energy content, density, and viscosity of Jet-A, *Fuel*, 2024, **358**, 129986.
5 J. Saavedra Lopez, R. A. Dagle, V. L. Dagle, C. Smith and K. O. Albrecht, Oligomerization of ethanol-derived propene and isobutene mixtures to transportation fuels: catalyst and process considerations, *Catal. Sci. Technol.*, 2019, **9**, 1117–1131.
6 M. Lilga, R. Hallen, K. O. Albrecht, A. Cooper, J. Frye and K. Ramasamy, Systems and processes for conversion of ethylene feedstocks to hydrocarbon fuels, USPTO, Battelle Memorial Institute, USA, 2018.
7 J. Heyne, B. Rauch, P. L. Clercq and M. Colket, Sustainable aviation fuel prescreening tools and procedures, *Fuel*, 2021, **290**, 120004.
8 J. Heyne, D. Bell, J. Feldhausen, Z. Yang and R. Boehm, Towards fuel composition and properties from Two-dimensional gas chromatography with flame ionization and vacuum ultraviolet spectroscopy, *Fuel*, 2022, **312**, 122709.
9 C. Faulhaber, C. Borland, R. Boehm and J. Heyne, Measurements of Nitrile Rubber Absorption of Hydrocarbons: Trends for Sustainable Aviation Fuel Compatibility, *Energy Fuels*, 2023, **37**, 9207–9219.
10 V. L. Dagle, G. Collinge, M. Rahman, A. Winkelman, W. Hu, J. Z. Hu, L. Kovarik, M. Engelhard, J. Jocz, Y. Wang, M.-S. Lee, V.-A. Glezakou, D. Ray, R. Rousseau and R. Dagle, Single-step conversion of ethanol into n-butene-rich olefins over metal catalysts supported on ZrO2-SiO_2 mixed oxides, *Appl. Catal., B*, 2023, **331**, 122707.
11 R. A. Dagle, A. D. Winkelman, K. K. Ramasamy, V. Lebarbier Dagle and R. S. Weber, *Ethanol as a renewable building block for fuels and chemicals*, Industrial & Engineering Chemistry Research, 2020.
12 Y. H. Lim, H. W. Ryu, Y. Hwang, K. Nam, J. Roh and D. H. Kim, Application of co-feeds in the catalytic conversion of light alkanes to aromatics: A comprehensive review, *ChemCatChem*, 2024, **16**, e202301456.
13 D. Liu, L. Cao, G. Zhang, L. Zhao, J. Gao and C. Xu, Catalytic conversion of light alkanes to aromatics by metal-containing HZSM-5 zeolite catalysts—A review, *Fuel Process. Technol.*, 2021, **216**, 106770.
14 Y. Nagamori and M. Kawase, Converting light hydrocarbons containing olefins to aromatics (Alpha Process), *Microporous Mesoporous Mater.*, 1998, **21**, 439–445.
15 Q. Zhou, S. Wang, Z. Wu, Z. Qin, M. Dong, J. Wang and W. Fan, Aromatization of n-C7–n-C9 alkanes on a Pt/KZSM-5 (deAl) catalyst, *Catal. Sci. Technol.*, 2023, **13**, 1009–1020.
16 S. M. Al-Zahrani, Catalytic Conversion of LPG to High-Value Aromatics: The Current State of the Art and Future Predictions, *Dev. Chem. Eng. Miner. Process.*, 2008, **6**, 101–120.
17 B. H. Davis, Alkane dehydrocyclization mechanism, *Catal. Today*, 1999, **53**, 443–516.
18 B. H. Davis, G. A. Westfall, J. Watkins and J. Pezzanite, Paraffin dehydrocyclization: VI. The influence of metal and gaseous promoters on the aromatic selectivity, *J. Catal.*, 1976, **42**, 247–256.
19 N. Y. Chen and T. Y. Yan, M2 forming - a process for aromatization of light hydrocarbons, *Ind. Eng. Chem. Process Des. Dev.*, 1986, **25**, 151–155.
20 P. D. Robert and A. Meyers, *UOP CYCLAR PROCESS*, McGraw-Hill Education, New York, 2016.
21 Y. He, U. Sanyal, M. Guo, H. Wang and K. K. Ramasamy, Catalyst Design for Efficient Olefin Aromatization: Insights into Metal-Promoted ZSM-5 Catalysts for Light and Heavy Olefin Conversion, *Ind. Eng. Chem. Res.*, 2025, **64**, 18553–18562.
22 T. Tsunoda and M. Sekiguchi, The Omega Process for Propylene Production by Olefin Interconversion, *Catal. Surv. Asia*, 2008, **12**, 1–5.
23 W. Liao, A. Nguyen and P. Liu, Alkali-induced catalytic tuning at metal and metal oxide interfaces, *Chem. Soc. Rev.*, 2025, **54**, 4164–4182.
24 Y. Jia, Q. Shi, J. Wang, C. Ding and K. Zhang, Synthesis, characterization, and catalytic application of hierarchical nano-ZSM-5 zeolite, *RSC Adv.*, 2020, **10**, 29618–29626.
25 Y.-J. Du, W.-D. Hu, C.-M. Wang, J. Zhou, G. Yang, Y.-D. Wang and W.-M. Yang, First-principles microkinetic analysis of Lewis acid sites in Zn-ZSM-5 for alkane dehydrogenation and its implication to methanol-to-aromatics conversion, *Catal. Sci. Technol.*, 2021, **11**, 2031–2046.
26 C. Perego and P. Ingallina, Recent advances in the industrial alkylation of aromatics: new catalysts and new processes, *Catal. Today*, 2002, **73**, 3–22.
27 S. A. Kishore Kumar, M. John, S. M. Pai, S. Ghosh, B. L. Newalkar and K. K. Pant, Selective hydroalkylation of benzene over palladium supported Y-Zeolite: Effect of metal acid balance, *Mol. Catal.*, 2017, **442**, 27–38.
28 ExxonMobil, *Hydroalkylation catalyst and process for use thereof*, ExxonMobil Chemical Patents Inc., United States, 2017, pp. 1–30.
29 I. B. Borodina, O. A. Ponomareva, F. Fajula, J. Bousquet and I. I. Ivanova, Hydroalkylation of benzene and ethylbenzene over metal containing zeolite catalysts, *Microporous Mesoporous Mater.*, 2007, **105**, 181–188.
30 J. Fahy, D. L. Trimm and D. J. Cookson, Four component catalysis for the hydroalkylation of benzene to cyclohexyl benzene, *Appl. Catal., A*, 2001, **211**, 259–268.
31 J. Huang, Z. Li, J. Yang, Z. Peng, Q. Liu and Z. Liu, Identification of Metal/Acid Matching Balance over Bifunctional Pd/Hβ toward Benzene Hydroalkylation, *Ind. Eng. Chem. Res.*, 2021, **60**, 2326–2336.
32 Z.-Q. Li, X. Fu, C. Gao, J. Huang, B. Li, Y. Yang, J. Gao, Y. Shen, Z. Peng, J.-H. Yang and Z. Liu, Enhancing the match-

ing of acid/metal balance by engineering an extra Si–Al framework outside the Pd/HBeta catalyst towards benzene hydroalkylation, *Catal. Sci. Technol.*, 2020, **10**, 1467–1476.
33 https://hypertextbook.com/facts/2003/EvelynGofman.shtml, last accessed April 8, 2025.
34 https://neutrium.net/articles/properties/specific-energy-and-energy-density-of-fuels/, last accessed April 8, 2025.
35 Z. Yang, Z. Xu, M. Feng, J. R. Cort, R. Gieleciak, J. Heyne and B. Yang, Lignin-based jet fuel and its blending effect with conventional jet fuel, *Fuel*, 2022, **321**, 124040.